

# Discrete Skeleton Evolution

Xiang Bai<sup>1</sup> and Longin Jan Latecki<sup>2</sup>

<sup>1</sup> Dept. of Electronics and Information Engineering, HuaZhong University of Science and Technology, Wuhan, Hubei 430074, China

xiang.bai@gmail.com

<sup>2</sup> Dept. of CIS, Temple University, Philadelphia, PA 19122, USA

latecki@temple.edu

**Abstract.** Skeleton can be viewed as a compact shape representation in that the shape can be completely reconstructed from the skeleton. We present a novel method for skeleton pruning that is based on this fundamental skeleton property. We iteratively remove skeleton end branches with smallest relevance for shape reconstruction. The relevance of branches is measured as their contribution to shape reconstruction. The proposed pruning method allows us to overcome the instability of skeleton representation: a small boundary deformation leads to large changes in skeleton topology. Consequently, we are able to obtain very stable skeleton representation of planar shapes.

**Keywords:** Skeleton, skeleton pruning, shape reconstruction from skeleton.

## 1 Introduction

Skeleton, or *Medial Axis*, has been widely used for shape analysis and object recognition, such as image retrieval and computer graphics, character recognition, image processing, and analysis of biomedical images [1]. Although a lot of efforts were made to analysis the shape based on the skeletal trees/graphs [16][17][23][24][25][28], these approaches have only demonstrated applicability to objects with simple and distinctive shapes, and therefore, cannot be applied to more complex shapes like shapes in the MPEG-7 data set [20]. There are two main factors that constraint the performance of skeleton-based shape matching: 1) skeleton's sensitivity to object's boundary deformation: little noise or variation of boundary often generates redundant skeleton branches that may disturb the topology of skeleton's graph seriously; 2) the time cost for extraction of skeleton and matching skeleton trees/graphs cannot satisfy the requirement of fast shape retrieval. The performance of skeleton matching depends directly on the property of shape representation. Therefore, to prune the grassy skeletons into the visual skeletons is usually inevitable [11]. The goal of this paper is to introduce a novel method for skeleton pruning, called Discrete Skeleton Evolution (DSE). The motivation of DSE is that removing the end branches of skeletons iteratively will not change the topology of the original shape, which benefits from the recent work of Bai et al. [19]. We obtained in a natural way a hierarchical structure of simplified skeletons as illustrated in Fig. 1.

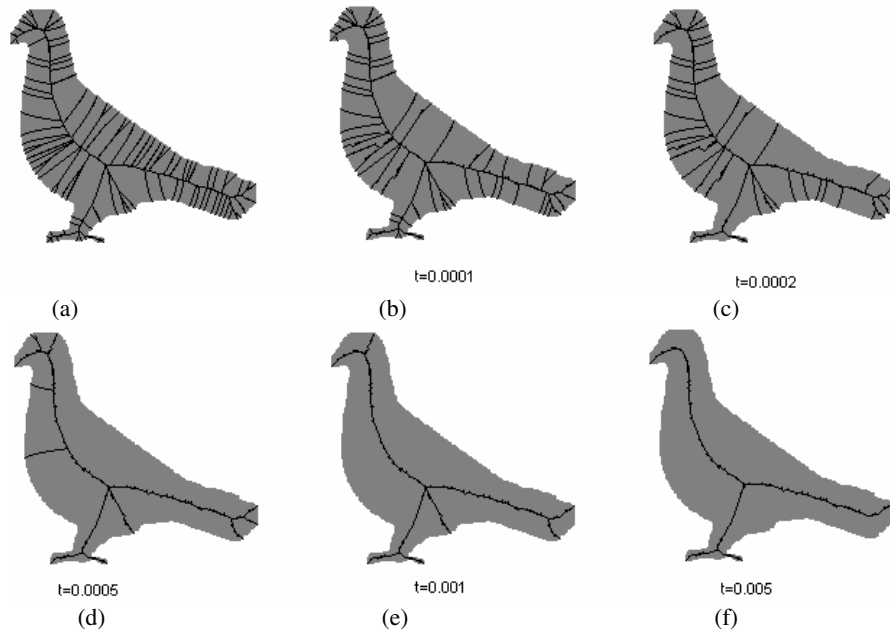


**Fig. 1.** The skeleton evolution process results in iterative pruning of the skeleton of a bird, (a) is the original skeleton and (b)~(f) are the pruned skeletons with the different thresholds

### 1.1 Related Work

Skeletonization approaches can be broadly classified into four types: thinning algorithms [5][6], discrete domain algorithms based on the Voronoi diagram [2][8][15], algorithms based on distance transform [3][4][7][9], and algorithms based on mathematical morphology [12][13][18].

All the obtained skeletons are subjected to the skeleton's sensitivity and many of them also include pruning methods along with the skeletonization. As an essential part of skeletonization algorithms, skeleton pruning algorithms usually appear in a variety of application-dependent formulations [11]. There are mainly two ways of pruning methods: (1) based on significance measures assigned to skeleton points [2][3], [11], [27], and (2) based on boundary smoothing before extracting the skeletons [11], [21]. In particular, curvature flow smoothing still have some significant problems that make the position of skeletons shift and have difficulty in distinguishing noise from low frequency shape information on the boundary [11]. A different kind of smoothing is proposed in [10]. A great progress have been made in the type (1) of pruning approaches that define a significance measure for skeleton points and remove points whose significance is low. Shaked and Bruckstein [11] give a complete analysis and compare such pruning methods. To the common significance measures of skeleton points belong to propagation velocity, maximal thickness, radius

function, axis arc length, the length of the boundary unfolded. Ogniewicz et al. [2] present a few significance measures for pruning hairy Voronoi skeletons without disconnecting the skeletons. Siddiqi et al. combine a flux measurement with the thinning process to extract a robust and accurate connected skeleton [22]. However, the error in calculating the flux is both limited by the pixel resolution and also proportional to the curvature of the boundary evolution front. This makes the exact location of endpoints difficult. Torsello et al. [18] overcome this problem by taking into account variations of density due to boundary curvature and eliminating the curvature contribution to the error. Recently, Bai et al. present a novel skeleton pruning method by dividing the contour into separate segments with the vertices from DCE (Discrete Curve Evolution) [19]. Since DCE does not change the topology, the pruned skeleton has the topology of the input skeleton.

## 2 Discrete Skeleton Evolution

Before we introduce the proposed approach, we give some definitions. According to Blum's definition of the medial axis [1], the skeleton  $S$  of a set  $D$  is the locus of the centers of maximal disks. A maximal disk of  $D$  is a closed disk contained in  $D$  that is interiorly tangent to the boundary  $\partial D$  and that is not contained in any other disk in  $D$ . Each maximal disc must be tangent to the boundary in at least two different points. With every skeleton point  $s \in S$  we also store the radius  $r(s)$  of its maximal disk.

By Theorem 8.2 in [26], the skeleton  $S$  is a geometric graph, which means that  $S$  can be decomposed into a finite number of connected arcs, called skeleton branches, composed of points of degree two, and the branches meet at skeleton joints (or bifurcation points) that are points of degree three or higher.

**Definition 1.** The skeleton point having only one adjacent point is an endpoint (the skeleton endpoint); the skeleton point having more than two adjacent points is a junction point. If a skeleton point is not an endpoint or a junction point, it is called a connection point. (Here we assume the curves of the skeleton is one-pixel wide)

**Definition 2.** A skeleton *end branch* is part of the skeleton between a skeleton endpoint and the closest junction point. Let  $l_i$  ( $i = 1, 2, \dots, N$ ) be the endpoints of a skeleton  $S$ . For each endpoint  $l_i$ ,  $f(l_i)$  denotes the nearest junction point. Formally, an *end branch*  $P(l_i, f(l_i))$  is the shortest skeleton path between  $l_i$  and  $f(l_i)$ .

For example, in Fig. 2, arc from 1 to  $a$  is a skeleton end branch:  $P(1, f(1)) = P(1, a)$ . The arc from  $a$  to  $b$  is not an end branch; it is a skeleton (inner) branch. Observe that point  $a$  is the nearest junction point of two endpoints (1 and 7).

Based on Blum's definition of a skeleton, a skeleton point  $s$  must be the center of a maximal disk/ball contained in the shape  $D$ .

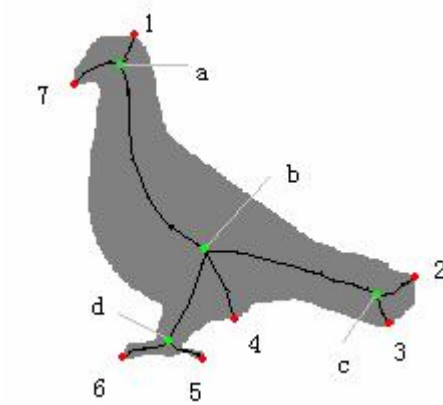


**Fig. 2.** The endpoints (red) and junction points (green) on the skeleton in Fig. 1(e)

**Definition 3.** Let  $r(s)$  denotes the radius of the maximal disk  $B(s, r(s))$  centered at a skeleton point  $s$ . The reconstruction of a skeleton  $S$  is denoted  $R(S)$  and given by

$$R(S) = \bigcup_{s \in S} B(s, r(s)) \tag{1}$$

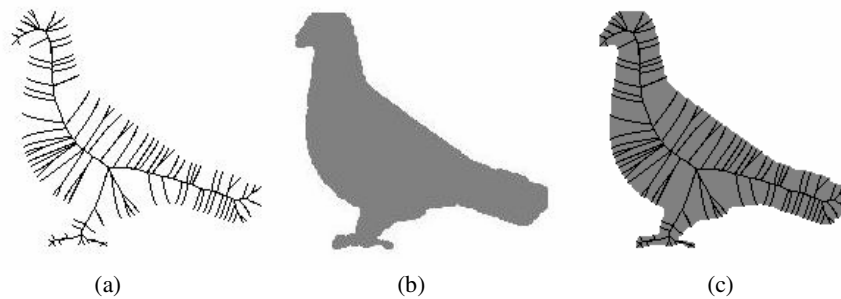


**Fig. 3.** The reconstruction (b) of the original skeleton (a) is very close to the original shape in (c)

As illustrated in Fig.3, we can reconstruct the original shape from its skeleton. Skeleton pruning can be seen as a simplification for skeleton, meanwhile, we hope the pruned skeleton can contain enough information of the shape.

In this paper, we introduce an iterative algorithm to prune the skeleton. In every step, we remove one end branch with the lowest weight. There are two motivations: 1) removing an end branch will not change the skeleton's topology; 2) the end branch with low contribution to the reconstruction is removed first.

We define the **weight**  $w_i$  for each end branch  $P(l_i, f(l_i))$  as:

$$w_i = 1 - \frac{A(R(S - P(l_i, f(l_i))))}{A(R(S))} \tag{2}$$

where function  $A(\cdot)$  is the area function. The intuition for skeleton pruning is that an end branch with a small weight  $w_i$  has a negligible influence on the reconstruction, since the area of the reconstruction without this branch is nearly the same as the area of the reconstruction with it. Therefore, it can be removed. The proposed skeleton pruning is based on iterative removal of end branches with the smallest weights until the desirable threshold is met.

The skeleton pruning algorithm is as follows:

1. We initialize the weights of all end branches  $w_i^{(0)}$  ( $i = 1, 2, \dots, N^{(0)}$ ) based on the original skeleton  $S^{(0)}$ :

$$w_i^{(0)} = 1 - \frac{A(R(S^{(0)} - P(l_i^{(0)}, f(l_i^{(0)})))}{A(R(S^{(0)}))} \tag{3}$$

2. In the  $k$ th iteration step, for  $i = 1, 2, \dots, N^{(k)}$  compute the weight for each end branch in the skeleton  $S^{(k)}$ :

$$w_i^{(k)} = 1 - \frac{A(R(S^{(k)} - P(l_i^{(k)}, f(l_i^{(k)})))}{A(R(S^{(k)}))} \tag{4}$$

3. Select the minimal weight  $w_{\min}^{(k)}$ . If  $w_{\min}^{(k)}$  is smaller than threshold  $t$ , go to 4; else, stop the evolution and output the  $S^{(k)}$  as the final result.
4. Remove end branch  $P_{\min}^{(k)}$  with the lowest weight  $w_{\min}^{(k)}$  and obtain the new skeleton:

$$S^{(k+1)} = S^{(k)} - P_{\min}^{(k)} \tag{5}$$

5. Set  $k=k+1$  and go to 2.

It is easy to see that this algorithm preserves the skeleton topology, since only end braches are removed. This fact is proven in Theorem 1, which states that  $S^{(k+1)}$  is topologically equivalent to the original skeleton  $S$ .

**Theorem 1.** For every  $k$ ,  $S^{(k+1)} = S^{(k)} - P_{\min}^{(k)}$  is a strong deformation retract of  $S$ .

**Proof:** We will show that  $S^{(k+1)}$ , is a strong deformation retract of  $S^{(k)}$ . Since composition of strong deformation retractions is a strong deformation retraction, it follows that  $S^{(k+1)}$ , is a strong deformation retract of  $S$ .

We obtain  $S^{(k+1)}$  by removing end branch  $P(l_{\min}, f(l_{\min}))$  from  $S^{(k)}$ . Therefore, mapping  $\pi: S^{(k)} \rightarrow S^{(k+1)}$  defined as identity on  $S^{(k+1)}$  and  $\pi(P(l_{\min}, f(l_{\min})))= f(l_{\min})$  is a strong deformation retraction. This proves the theorem.

The robustness to noise and other boundary deformations of the proposed method follows from the fact that we compare the area. As it is well known, even significant contour noise has very small effect on the object area. We will demonstrate this fact in Section 3.1. Moreover, the area of articulated parts remains nearly constant, which makes the proposed skeleton pruning robust for articulated objects. For example, the obtained skeletons of the classes of Glas and Elephant in Fig.5 are with clear structures and insensitive to the boundary protrusions. Observe also that our approach does not shorten the remaining skeleton branches, since we only completely remove end branches. This is a desirable feature for object recognition, which we illustrate in Section 3.2.

### 3 Experiments and Discussions

In this section, we evaluate the performance of the proposed method in three parts. In Section 3.1, we demonstrate the stability to shape deformations and contour noise; In Section 3.2, we provide a comparison to other methods. In Section 3.3, we show that the proposed method is independent from the topology of the skeleton. This is in accord with Theorem 1, which guarantees topology preservation even in the presence of multiple loops.

#### 3.1 Test on Kimia's Dataset

In this Section, we want to demonstrate the robustness to shape deformations and noise. We apply the proposed method to a well-known dataset for shape analysis

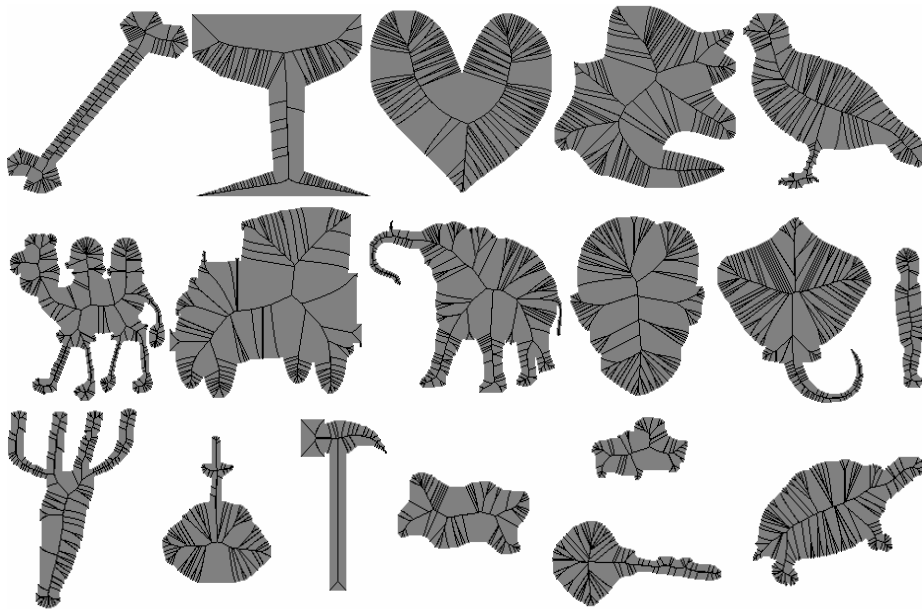
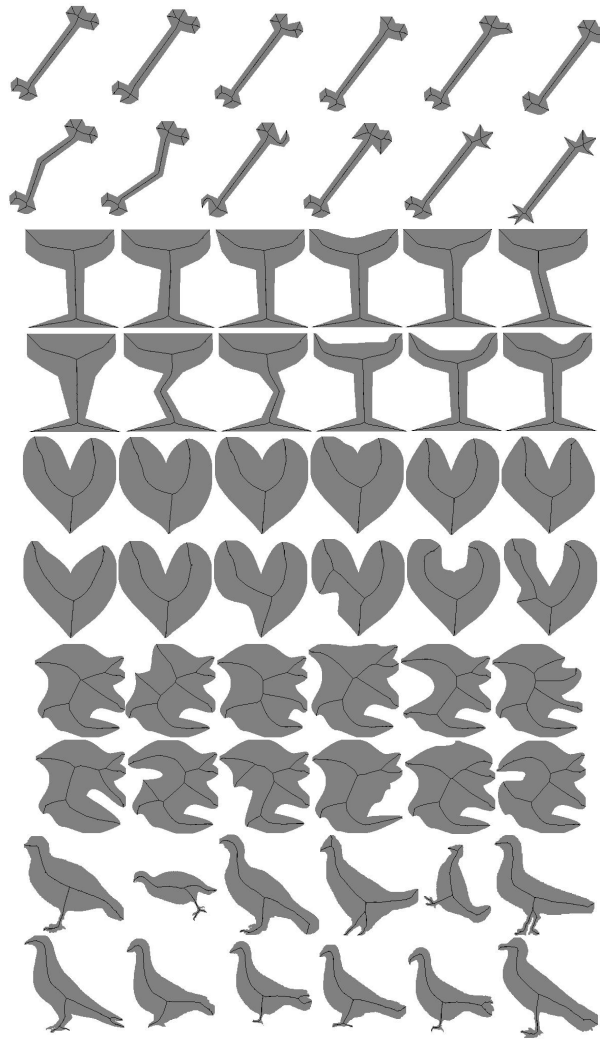


Fig. 4. Sample shapes in Kimia's dataset with original skeletons

(Kimia's 216 shapes), which consists of 18 classes with 12 shapes in each class [16]. The shapes in the same class are similar but slightly different, and the original skeletons are very grassy due to the many small noises or changes on their boundary as shown in Fig.4. We use the same threshold  $t$  for the shapes in the same class, and the values of  $t$  for all the classes are listed in Table.1. We put all the results in Fig.5. The obtained pruned skeletons in Fig.5 seem to be in accord with human perception and stable to the threshold  $t$ , which can be used for skeleton-based shape analysis efficiently.



**Fig. 5.** The pruned skeletons of Kimia's dataset

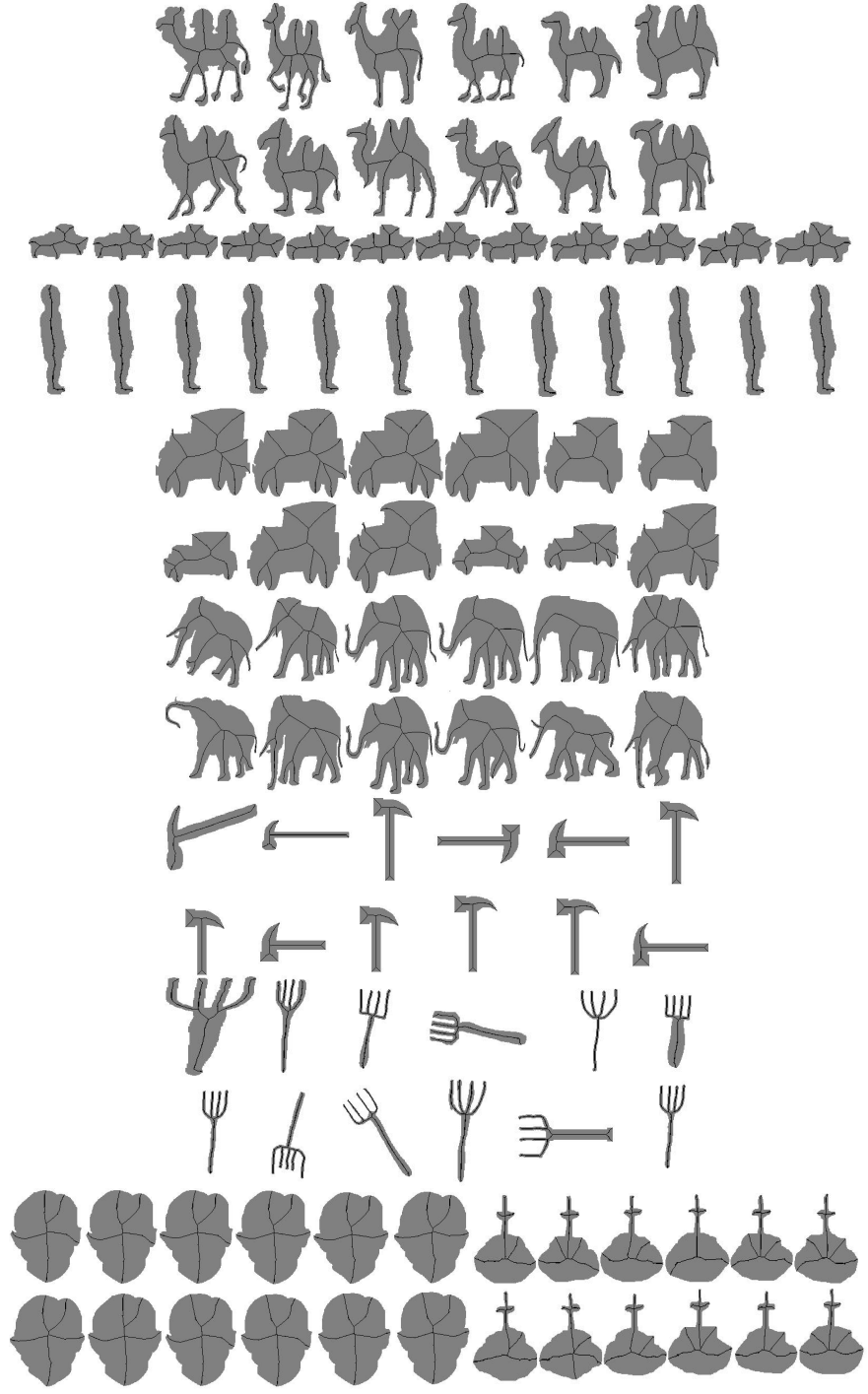


Fig. 5. (continued)



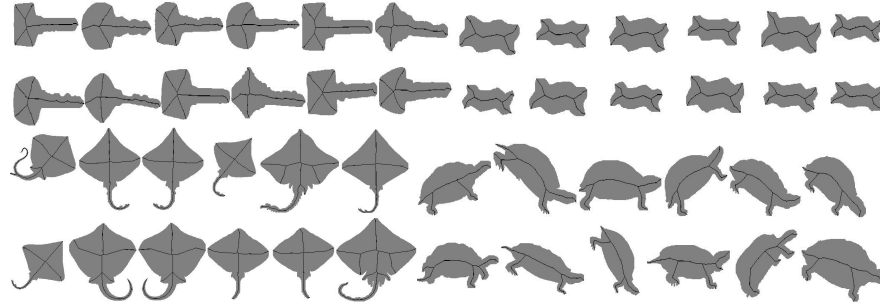


Fig. 5. (continued)

Table 1. The values of  $t$  used in our experiments on Kimia’s 18 classes

Class	Bone	Glas	Heart	Misk	Bird	Brick
Threshold	0.0015	0.005	0.005	0.005	0.005	0.010
Class	Camel	Car	Children	Classic	Elephant	Face
Threshold	0.005	0.004	0.010	0.004	0.004	0.008
Class	Fork	Fountain	Hammer	Key	Ray	Turtle
Threshold	0.005	0.006	0.005	0.005	0.005	0.007

### 3.2 Comparison with Other Methods

We compare our result with two recent publications: 1) Torsello’s modified Hamilton Jacob Skeleton [18]; 2) Bai’s pruned skeleton by contour partitioning with DCE [19].

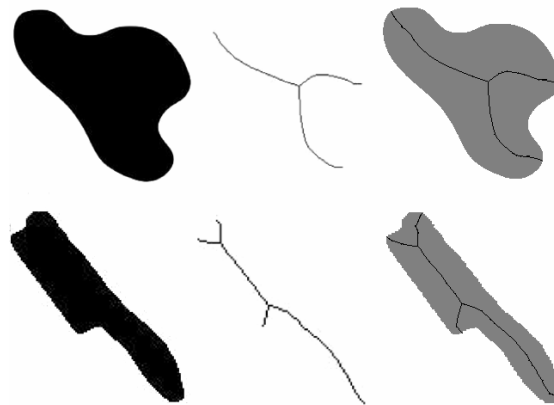


Fig. 6. Comparison with Torsello’s results in [18]: column (a) are the example original shapes, column (b) are Tosello’s results, and column (c) are our results by DSE

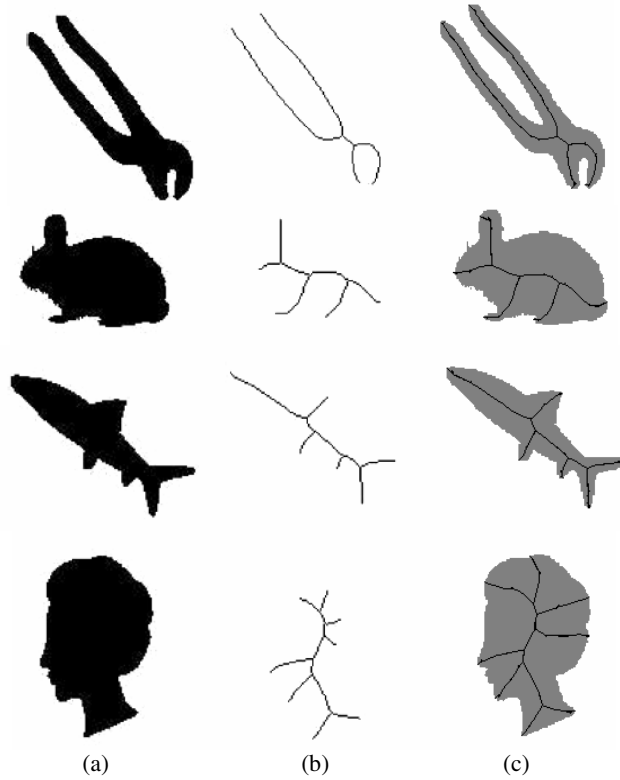


Fig. 6. (continued)

We test our algorithm on several representative shapes in Torsello’s paper [18]. In Fig.6, it’s easy to observe that our results are comparable to Torsello’s results, and all the results are computed with the same  $t$  ( $t = 0.005$ ). In addition, our method never shortens the skeleton branches. For example, in Torsello’s results, some skeleton branches of women’s head are much shorter than our result.

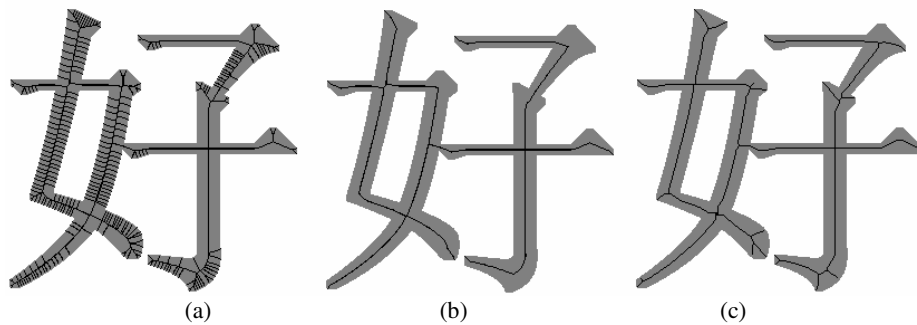


Fig. 7. Comparison with Bai’s result in [19]

We also compare our result with pruning result by DCE in [19]. As shown in Fig. 7, we can observe that the results of two methods are very close with clear structure, but our result (when  $t = 0.005$ ) in Fig. 7(b) is more stable to the small protrusions, such as the short branches ended at the legs of the camel in Fig. 7(a). The reason for solving this problem is that our method is based on skeletons directly.

### 3.3 Test on Skeletons with Loops

In this section, we show the performance of the proposed method on the images with holes. Fig. 8 gives the skeletons of a Chinese character. Our pruned skeleton in Fig. 8 (b) is better than the thinning result (c) obtained with a morphological thinning. An example in [19] is also performed by the proposed algorithm in Fig. 9, and the pruned results in Fig. 9(b) and Fig. 9(c) demonstrate that our method is topology preserved.



**Fig. 8.** The Skeletons of a Chinese character. (a) and (b) is the original skeleton and the pruned skeleton separately, and (c) is the result of morphological thinning.

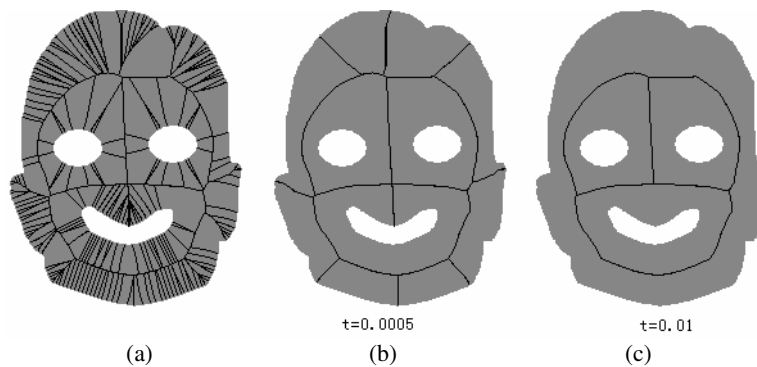


**Fig. 9.** The skeletons of a face in [19]. (a) is the original skeleton, (b) and (c) are the pruned results with different thresholds.

### 3.4 Some Experimental Details

All the original skeletons in this paper were generated based on the distance transform by the algorithm in [4]. Our pruning algorithm is with high time cost due to the reconstruction in every iterative step, and the average time for pruning a noisy skeleton is about 4 minutes on the PC with 1.5 GHZ CPU and 512M RAM. Therefore, for increasing speed, another way is encouraged: First, prune the skeletons with the pruning algorithm in [19] in the coarse level; then, prune the pruned skeletons from algorithm [19] with the proposed algorithm. In this way, the average time cost for one pruning has been reduced to about 15 seconds.

## 4 Conclusions and Future Work

We present an iterative algorithm for pruning skeleton that is based on removing the end branch with the lowest weight for reconstruction in each step. The experiments prove that DSE is an efficient tool for skeleton-based representation and recognition. Even for different shapes of the same class in Kimia's dataset, we can use the same threshold, which is very important for automatic recognition with skeletons. Moreover, we have proved that DSE is topology preserved both in theorem and experiment. In the future, our work will focus on pruning 3D curve skeletons in analogous way.

**Acknowledgments.** We want to thank Zhuowen Tu for his useful comments and suggestions on this work. This work was supported by the Cultivating Fond for Momentous Scientific Innovation Project of Higher Education in China (Grant no. 705038) and in part by the NSF Grant IIS-0534929 and by DOE Grant DE-FG52-06NA27508.

## References

1. Blum, H.: Biological Shape and Visual Science (Part I). *J. Theoretical Biology* 38, 205–287 (1973)
2. Ogniewicz, R.L., Kübler, O.: Hierarchic Voronoi skeletons. *Pattern Recognition* 28(3), 343–359 (1995)
3. Malandain, G., Fernandez-Vidal, S.: Euclidean skeletons. *Image and Vision Computing* 16, 317–327 (1998)
4. Choi, W.-P., Lam, K.-M., Siu, W.-C.: Extraction of the Euclidean skeleton based on a connectivity criterion. *Pattern Recognition* 36, 721–729 (2003)
5. Pudney, C.: Distance-Ordered Homotopic Thinning: A Skeletonization Algorithm for 3D Digital Images. *Computer Vision and Image Understanding* 72(3), 404–413 (1998)
6. Leymarie, F., Levine, M.: Simulating the grassfire transaction form using an active Contour model. *IEEE Trans. Pattern Analysis and Machine Intell.* 14(1), 56–75 (1992)
7. Golland, P., Grimson, E.: Fixed topology skeletons. In: *CVPR*, vol. 1, pp. 10–17 (2000)
8. Mayya, N., Rajan, V.T.: Voronoi Diagrams of polygons: A framework for Shape Representation. In: *Proceedings of the IEEE Conference on Computer Vision and Pattern Recognition*, pp. 638–643 (1994)

9. Ge, Y., Fitzpatrick, J.M.: On the Generation of Skeletons from Discrete Euclidean Distance Maps. *IEEE Trans. Pattern Analysis and Machine Intell.* 18(11), 1055–1066 (1996)
10. Gold, C.M., Thibault, D., Liu, Z.: Map Generalization by Skeleton Retraction. In: *ICA Workshop on Map Generalization*, Ottawa (August 1999)
11. Shaked, D., Bruckstein, A.M.: Pruning Medial Axes. *Computer Vision and Image Understanding* 69(2), 156–169 (1998)
12. Dimitrov, P., Damon, J.N., Siddiqi, K.: Flux Invariants for Shape. In: *Int. Conf. Computer Vision and Pattern Recognition* (2003)
13. Siddiqi, K., Bouix, S., Tannenbaum, A.R., Zucker, S.W.: Hamilton-Jacobi Skeletons. *International Journal of Computer Vision* 48(3), 215–231 (2002)
14. August, J., Siddiqi, K., Zucker, S.W.: Ligature Instabilities and the Perceptual Organization of Shape. *Computer Vision and Image Understanding* 76(3), 231–243 (1999)
15. Brandt, J.W., Algazi, V.R.: Continuous skeleton computation by Voronoi diagram. *Comput. Vision, Graphics, Image Process* 55, 329–338 (1992)
16. Sebastian, T.B., Klein, P.N., Kimia, B.B.: Recognition of shapes by editing their shock graphs. *IEEE Trans. Pattern Anal. Mach. Intell.* 26(5), 550–571 (2004)
17. Aslan, C., Tari, S.: An Axis-Based Representation for Recognition. *ICCV*, pp. 1339–1346 (2005)
18. Torsello, A., Hancock, E.R.: Correcting Curvature-Density Effects in the Hamilton-Jacobi Skeleton. *IEEE Transaction on Image Processing* 15(4), 877–891 (2006)
19. Bai, X., Latecki, L.J., Liu, W.Y.: Skeleton Pruning by Contour Partitioning with Discrete Curve Evolution. *IEEE Trans. Pattern Anal. Mach. Intell.* 29(3), 449–462 (2007)
20. Latecki, L.J., Lakämper, R., Eckhardt, U.: Shape Descriptors for Non-rigid Shapes with a Single Closed Contour. In: *Proc. of IEEE Conf. on Computer Vision and Pattern Recognition (CVPR)*, pp. 424–429 (2000)
21. Mokhtarian, F., Mackworth, A.K.: A Theory of Multiscale, Curvature-Based Shape Representation for Planar Curves. *IEEE Trans. Pattern Analysis and Machine Intelligence* 14, 789–805 (1992)
22. Dimitrov, P., Phillips, C., Siddiqi, K.: Robust and Efficient Skeletal Graphs. In: *Proc. IEEE Conf. Computer Vision and Pattern Recognition*, pp. 1417–1423 (2000)
23. Demirci, F., Shokoufandeh, A., Keselman, Y., Bretzner, L., Dickinson, S.: Object Recognition as Many-to-Many Feature Matching. *International Journal of Computer Vision* 69(2), 203–222 (2006)
24. Siddiqi, K., Shokoufandeh, A., Dickinson, S.J., Zucker, S.W.: Shock Graphs and Shape Matching. *International Journal of Computer Vision* 35(1), 13–32 (1999)
25. Zhu, S.C., Yuille, A.L.: FORMS: A flexible object recognition and modeling system. *Int. J. Comput. Vis. (IJCV)* 20(3), 187–212 (1996)
26. Choi, H.I., Choi, S.W., Moon, H.P.: Mathematical Theory of Medial Axis Transform. *Pacific J. Math.* 181(1), 57–88 (1997)
27. van Eede, M., Macrini, D., Telea, A., Sminchisescu, C., Dickinson, S.: Canonical Skeletons for Shape Matching. *ICPR*, 64–69 (2006)
28. Tu, Z., Yuille, A.L.: Shape Matching and Recognition Using Generative Models and Informative Features. In: Pajdla, T., Matas, J(G.) (eds.) *ECCV 2004*. LNCS, vol. 3021, pp. 195–209. Springer, Heidelberg (2004)